

Comparative analysis of the photocatalytic removal of methylene blue and pyrene on TiO₂ and WO₃/TiO₂ particles

Joseph Albert Mendoza^a, Dong Hoon Lee^b, Joo-Hyon Kang^{b,*}

^aSchool of Chemical, Biological, Materials Engineering and Sciences, Mapua University, 658 Muralla St., Intramuros, Manila, Philippines

^bDepartment of Civil and Environmental Engineering, Dongguk University – Seoul, 30 Pil-dong-ro 1-gil, Jung-gu, Seoul, Republic of Korea, email: joohyon@dongguk.edu (J.-H. Kang)

Received 3 January 2020; Accepted 3 March 2020

ABSTRACT

This study investigated the performance of ultraviolet (UV) light active TiO₂ and UV-visible light active WO₃/TiO₂ nanoparticles coated on zeolite for degrading organic pollutants such as methylene blue and pyrene. Using glass dishes for the batch photocatalytic removal experiments of the organic pollutants, the removal efficiencies of methylene blue and pyrene by two different photocatalytic particles coated on natural zeolites were evaluated. The results showed that the TiO₂ and WO₃/TiO₂-coated zeolites are excellent photoactive materials providing enhanced removal function (>95% removal efficiency of methylene blue) under UV and UV-visible light irradiation, respectively. However, lower efficiencies were observed for both TiO₂ and WO₃/TiO₂ powders and TiO₂ and WO₃/TiO₂-coated zeolite in removing pyrene in aqueous solution under UV and visible light irradiation. In column tests, both TiO₂ and WO₃/TiO₂-coated zeolites have shown only measurable pyrene removal efficiency of ~50% under UV irradiation. This could be due to the negligible adsorption of pyrene on the photocatalytic reaction sites both for TiO₂ and WO₃/TiO₂-coated zeolite. Nevertheless, this study revealed the potential utility of photocatalytic particles in improving urban water quality, which can be utilized in the form of the surface component for various urban infrastructures.

Keywords: Nanoparticles; Organics; Photocatalysis; WO₃/TiO₂; Zeolite

1. Introduction

Organic pollutants such as methylene blue and polycyclic aromatic hydrocarbons (PAHs) are being discharged in large amounts from various anthropogenic sources such as industrial complexes, which are toxic and non-biodegradable and can trigger contaminations in various natural water bodies if left untreated.

Organic dyes such as methylene blue, rhodamine B, acid red, and ethyl violet are usually found in textile processing industries generated from the dyeing, bleaching, and washing processes [1,2]. Wastewaters discharged from textile industries are toxic to the environment due to their high

biological oxygen demand and chemical oxygen demand. Dyes are soluble in water even in small amounts which could affect visibility and transparency of the water bodies resulting in decreased photosynthesis perturbing the marine ecosystem and could cause eutrophication [3]. They are also considered to be mutagens and carcinogens thus prompting their removal from industrial effluents.

PAHs are comprised of fused aromatic benzene rings having nonpolar nature with high desorption activation energy. PAHs are persistent compounds in the environment due to their chemically stable structure and low bioavailable fraction.

* Corresponding author.

PAHs are categorized as low molecular weight (LMW) and high molecular weight (HMW) PAHs based on molecular structure. The LMW PAHs include two and three rings structure while HMW PAHs comprise four and more rings structure and the aqueous solubility of PAHs decrease almost linearly with an increase in molecular mass. Although there are more than 100 different types of PAHs, only 16 PAHs are on the priority list of the U.S. Environmental Protection Agency (US EPA) due to their negative impact on the environment and human health [4].

Among the promising techniques to degrade such pollutants is photocatalysis under UV-visible light irradiation which does not require excessive chemical reagents and will only need the solar spectra and/or indoor illuminations for it to function. Photocatalysis is a process that utilizes ultraviolet (UV) and visible light radiation from sunlight or artificial light assisting in breaking down different substances including organic materials and inorganic molecules. TiO_2 has been reported as an efficient photocatalyst for degrading organic pollutants due to its stability and nontoxicity [5] but TiO_2 only absorbs wavelengths at the ultraviolet (UV) light region, and recent researches have been focused on developing newer photocatalysts that absorb visible light.

Among the methods to make TiO_2 absorb visible light is to introduce dopants such as metals (e.g. Cd, Au, Pt, Cu, etc.), non-metals (e.g. Br, N, C, B, F, etc.), and other metal oxides (e.g. WO_3 , BiO , ZnO , CuO , Fe_2O_3 , etc.) [6,7]. Composites of WO_3/TiO_2 have been reported to efficiently absorb visible light and generate hydrogen from water splitting process [8]. However, limited studies have reported on its use in the degradation of organic pollutants such as PAHs and methylene blue.

The objective of this study is to explore the effectiveness of WO_3/TiO_2 photocatalytic particles and coated zeolite, synthesized from previous research [9], in the photocatalytic removal of methylene blue and pyrene in aqueous solutions, and comparatively analyze their removal efficiencies.

2. Material and methods

2.1. Batch photocatalytic removal of methylene blue and pyrene

The batch kinetic studies were performed based on the ISO standard 10678:2010 [10] which is the standard method for studying photocatalytic degradation of methylene blue. The schematic illustration of the batch test performed is shown in Fig. 1a. The ease of performing the experiment and the small thickness of the petri dish used can provide an appropriate measurement of the photocatalytic performance of WO_3/TiO_2 particles and WO_3/TiO_2 coated zeolite in removing PAHs such as pyrene, and methylene blue.

The degradation experiments were performed by preparing 100 mL of 15.0 ppm of the methylene blue solution (1.0 ppm for pyrene), and 0.10 g of the photocatalyst (i.e. TiO_2 , WO_3/TiO_2) is added into the solution. For the case of coated zeolite, 20 g was added covering the entire bottom surface of the petri dish.

The Petri dishes could equilibrate in the dark for at least 1 h. The length of time in the dark was based on the adsorption tests performed where different concentrations (5, 10, 20 ppm for methylene blue; 5, 2, 0.5 ppm for pyrene) for

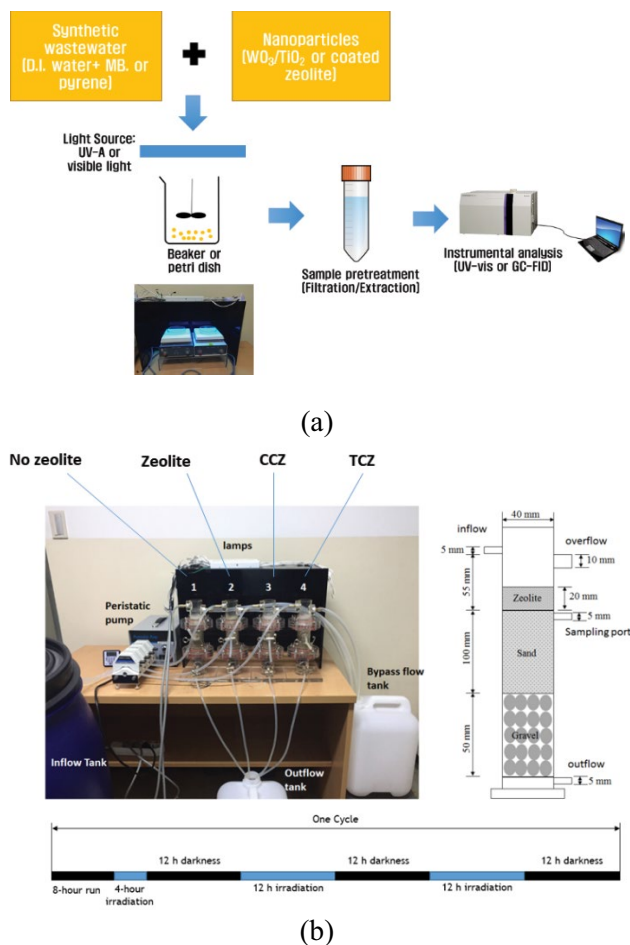


Fig. 1. (a) Batch test schematic for the photocatalytic removal of methylene blue and pyrene and (b) column test schematic for the photocatalytic removal of methylene blue and pyrene.

various photocatalysts were tested without a light source. And then the light source (UV A, blacklight, 20 W Sankyo Denki, Japan, or white fluorescent lamp, Osram, Germany; 6 pcs) was turned on, placed above the solution, and exposed for 1 h. During the exposure time, a 5 mL sample was extracted and filtered with a syringe filter from the solution after specific time intervals (0, 15, 30, 45, 60 min) and transferred to a conical tube. The conical tube was shaken to mix the solution inside. For methylene blue, the samples were analyzed immediately for its absorbance using a UV-Vis spectrometer UV-1650PC (Shimadzu, Japan). While for pyrene, samples were pretreated initially through solid-phase extraction, which is described in detail in the next section, and then analyzed using gas chromatography with flame ionization detector (GC-FID) using the parameters listed in Table 1 (Agilent 6890N, USA).

2.2. Column tests for the photocatalytic removal of aqueous pyrene

Column tests for the removal of pyrene using coated zeolite were performed. Four columns (I.D. = 4 cm; H = 22 cm) made from transparent acryl were prepared. Gravel, sand, and coated zeolite were placed in the column according

Table 1
GC–FID parameters for pyrene analysis

Parameter	Condition
Injection (sample) volume	1 μ L
Carrier gas	Helium (He)
Gas flow rate (He)	104.6 mL/min
Pressure (He)	70 kPa
Linear velocity (He)	35 cm/s
Injection mode	Splitless
Temperatures	
• Inlet	300°C
• Initial oven temperature	50°C
• Oven heating rate	10°C/min
• Final oven temperature	300°C
• Detector (FID)	300°C
Detection limit	10 ppb

to the following height: coated zeolite: 2 cm; sand: 10 cm; gravel: 5 cm. The first column was a blank made up of only sand and gravel. While the second column contained natural zeolite. The third and fourth column contained the WO_3/TiO_2 and TiO_2 coated zeolite, respectively. The light source (UV-A, Sankyo Denki, 6 pcs.) were placed at the topmost portion of the column frame. The schematic and actual setup were shown in Fig. 1b.

Synthetic wastewater was made by mixing 200 mL of 1,000 ppm stock solution of pyrene into a 20 L container to produce 10 ppm. The stock solution was made by dissolving 1.0 g of pyrene in 1,000 mL acetonitrile and sonicated for 60 min. The synthetic wastewater was introduced into the column with a peristaltic pump operating constantly at 35 rpm (20 ± 2 mL/min). Samples were taken at the following time intervals: 1, 4, and 8 h. Samples were pre-treated and extracted within 24 h using solid-phase extraction disks (C18, 3M, Empore, EEPA method 3535A [11]). After the 8 h cycle was completed, the light source was turned on for 4 h. Then, the columns were dried for 2 d before starting another 8 h cycle of operation. Another test was performed using a lower concentration of pyrene (1.0 and 0.10 ppm).

The solid-phase extraction method used in pre-treating and recovering pyrene from the water was based on the U.S. EPA method 3535A using a hydrophobic extraction disk to be fitted on the standard vacuum filtration setup. Briefly, the method consisted of three phases: disk conditioning, sample extraction, and sample elution. Before the conditioning phase, the extraction disk was pre-wetted by pouring approximately 20 mL of acetonitrile (elution solvent) to the filter reservoir and vacuum was applied until the disk was dry. Then, on the conditioning step, approximately 20 mL of methanol was added on the filter cap, and a vacuum was applied until a thin layer (~3 mm) of the solvent remained at the top of the filtration disk. It was soaked in methanol for 30 s, then 20 mL of deionized water was added, and a vacuum was applied until a thin layer remains at the top of the disk. Then, the sample was poured into the filter reservoir and vacuum was applied until the disk was dry. The supernatant liquid in the Erlenmeyer

flask was discarded, and a test tube was placed to collect the sample to be eluted. The sample was first soaked in 10 mL acetonitrile for 30 s before applying a vacuum to flush the samples out of the extraction disk. And another 10 mL acetonitrile was poured on the sample to have a total eluted sample volume of 20 mL. The eluted samples were analyzed using GC–FID.

3. Results and discussion

3.1. Adsorption studies on methylene blue and pyrene

Adsorption experiments for methylene blue and pyrene were conducted using the batch method described by ISO 10678:2010 but without light irradiation. Figs. 2 and 3 show the adsorption of pyrene with varying concentrations into TiO_2 powders and TiO_2 coated zeolite, respectively. The corresponding isotherm is also shown and pyrene adsorption on TiO_2 satisfies the Langmuir adsorption isotherm. Fig. 3 revealed that pyrene adsorption equilibrium could have started at 4 h verified by the Langmuir isotherm having a relatively good fit using the final equilibrium points. However, upon the calculation of monolayer adsorption of pyrene per mass of catalyst (q_m), TiO_2 powders have

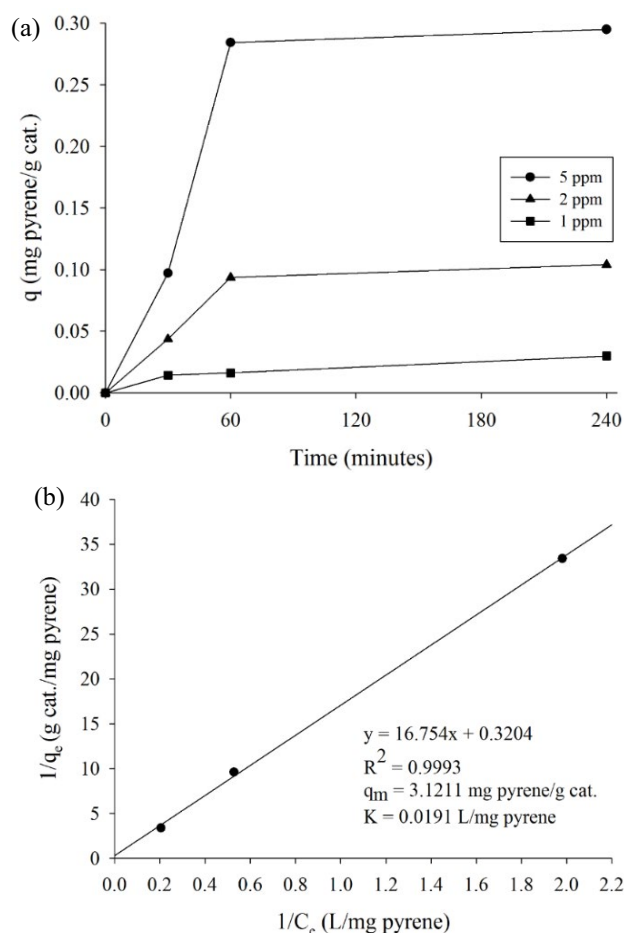


Fig. 2. (a) Adsorption of pyrene with varying concentrations on TiO_2 powders under dark conditions and (b) the corresponding Langmuir adsorption isotherm.

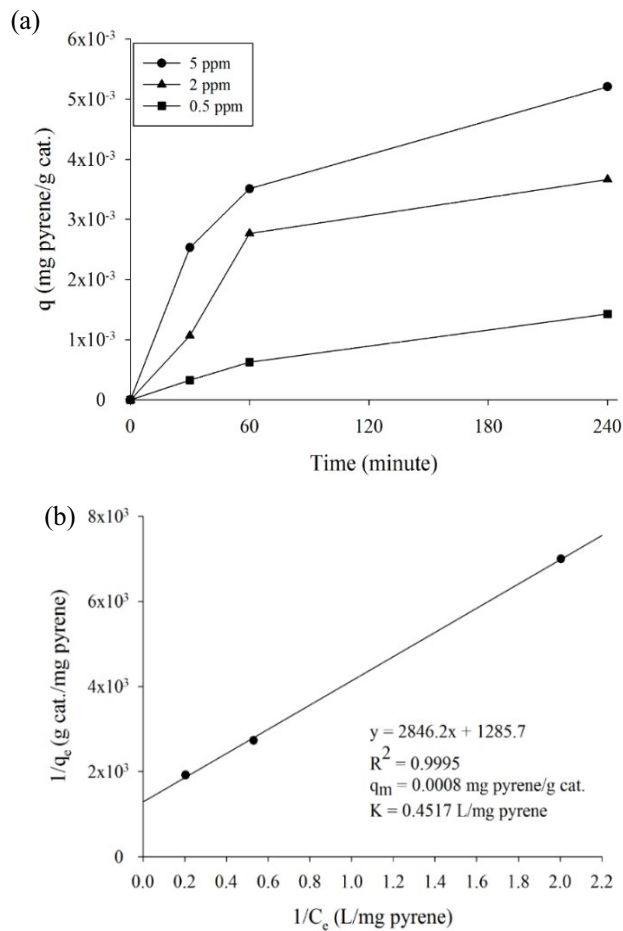


Fig. 3. (a) Adsorption of pyrene with varying concentrations on TiO_2 coated zeolite under dark conditions and (b) the corresponding Langmuir adsorption isotherm.

adsorbed pyrene more efficiently than the TiO_2 coated zeolite. This could be due to the molecular size of pyrene which could be larger than the pore sizes of zeolite.

Figs. 4 and 5 show the adsorption results for pyrene into WO_3/TiO_2 powders and WO_3/TiO_2 coated zeolite. A similar trend has been observed that the WO_3/TiO_2 powders have adsorbed pyrene more efficiently than their corresponding coated zeolite. The adsorption isotherms for both WO_3/TiO_2 powders and WO_3/TiO_2 coated zeolite have a good fit with the Langmuir equation [3,5] as shown by the coefficient of variance (R^2) in Figs. 4 and 5.

Meanwhile, methylene blue (MB) with similar polycyclic aromatic configuration with pyrene has shown better adsorption with TiO_2 and WO_3/TiO_2 powders and TiO_2 and WO_3/TiO_2 -coated zeolite. The monolayer of methylene blue adsorbed per mass of catalyst (q_m) was greater than that of pyrene as shown in Table 2 suggesting efficient adsorption of MB on the surface of catalysts. The efficient adsorption of MB could be due to the cationic nature of MB on the aqueous solution and whereas the catalyst surface is predominantly more electronegative and thus adsorption could be due to electrostatic interactions which could be absent between pyrene and the catalysts.

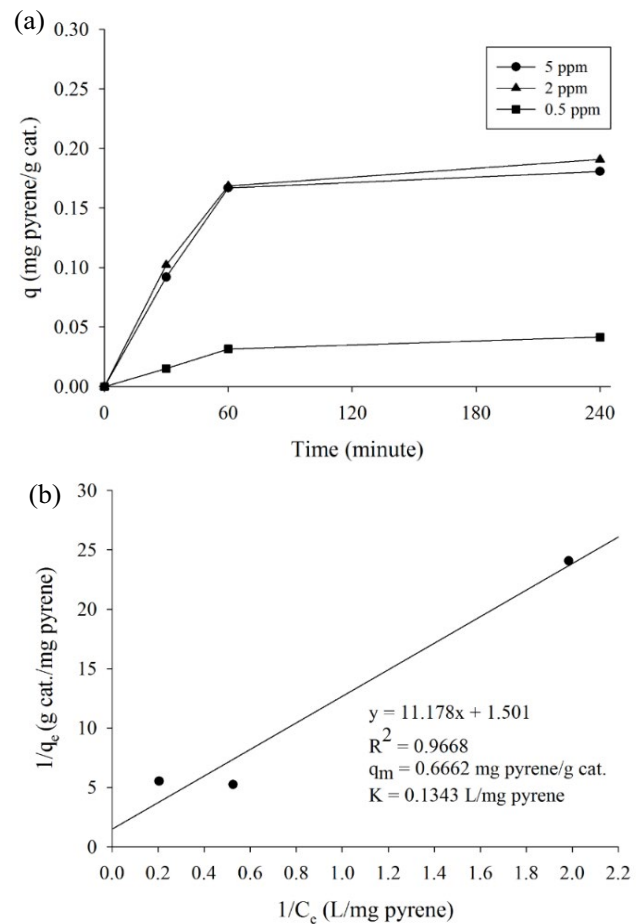


Fig. 4. (a) Adsorption of pyrene with varying concentrations on WO_3/TiO_2 powders under dark conditions and (b) the corresponding Langmuir adsorption isotherm.

3.2. Batch photocatalytic removal of methylene blue and pyrene

Figs. 6 and 7 show the concentration profile of the photocatalytic removal of pyrene using TiO_2 powder and TiO_2 -coated zeolite, respectively under UV irradiation. The removal of pyrene is generally faster on the TiO_2 coated zeolite than with TiO_2 powders only. This could be due to the greater formation of OH radicals generated [12] through the hole oxidation on the photocatalyst surface reacting with water adsorbed by zeolite. It is known that zeolite has a high affinity for water molecules making zeolite among the most widely used moisture adsorbent in various industries. The OH radicals, produced from photocatalysis, had effectively oxidized and rapidly removed pyrene from the aqueous solution. Furthermore, the removal is enhanced by the photocatalytic generation of electrons from TiO_2 aiding in the mineralization of pyrene; and the products could have been adsorbed on the free surface of the zeolite.

Figs. 8 and 9 show the concentration profile of the photocatalytic removal of pyrene using the composite WO_3/TiO_2 powders and WO_3/TiO_2 coated zeolite, respectively under visible light irradiation. It can be seen also that the photocatalytic reaction proceeds faster on the WO_3/TiO_2 coated zeolite

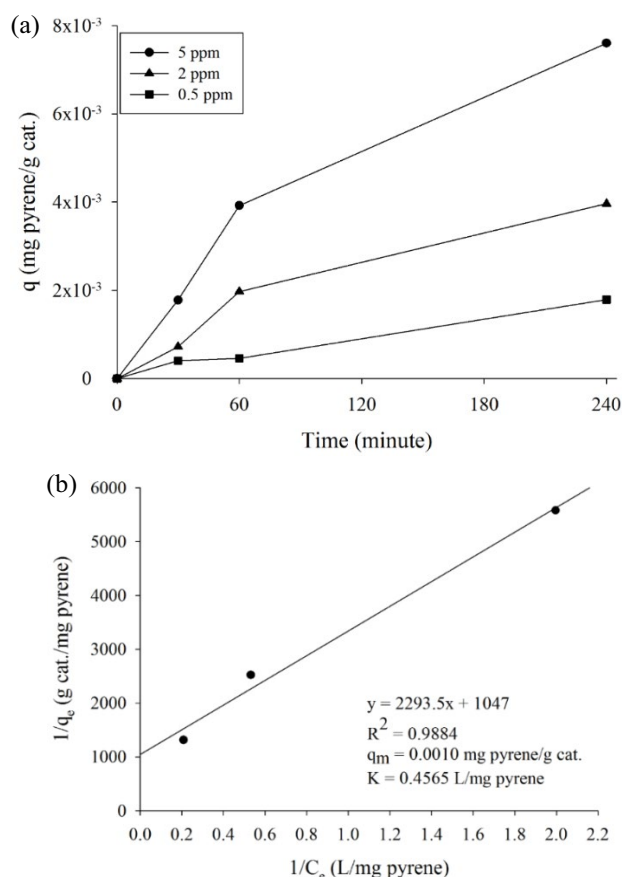


Fig. 5. (a) Adsorption of pyrene with varying concentrations on WO_3/TiO_2 coated zeolite under dark conditions and (b) the corresponding Langmuir adsorption isotherm.

Table 2
Comparative values of the adsorption capacity for methylene blue and pyrene

Catalyst type	q_m (g MB/g cat.)	q_m (g pyrene/g cat.)
TiO_2 powders	5.3277	3.1211
WO_3/TiO_2 powders	7.3529	0.6662
TiO_2 coated zeolite	0.0673	0.0008
WO_3/TiO_2 coated zeolite	0.5516	0.0010

than compared to the WO_3/TiO_2 powders. The removal mechanism for pyrene on WO_3/TiO_2 could be similar to that of using TiO_2 following first-order reaction kinetics because of the good fit observed when plotting $\ln(C/C_0)$ with respect to time. However, photocatalytic reactions for WO_3/TiO_2 powders and WO_3/TiO_2 coated zeolite are slower than compared to the TiO_2 and TiO_2 coated zeolite resulting in lower removal efficiencies which could be due to the lower photon energy emitted by visible light than UV irradiation. Therefore, it can be deduced that pyrene requires higher photon energy (i.e. UV light) to be efficiently degraded photocatalytically.

Table 3 shows the removal efficiencies of pyrene and methylene blue for the various photocatalysts used under

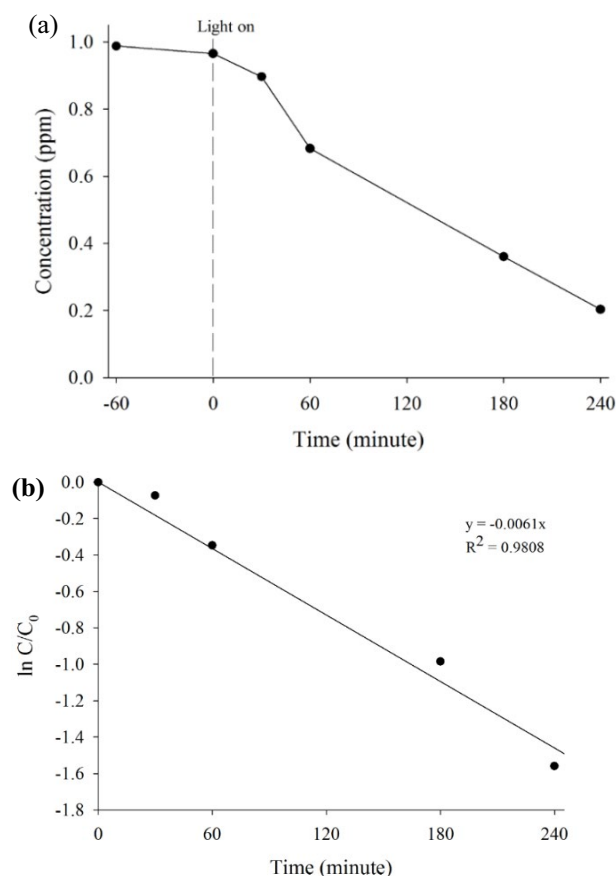


Fig. 6. (a) Concentration profile of the photocatalytic removal of pyrene using TiO_2 powders and (b) reaction kinetics of the photocatalytic removal of pyrene using TiO_2 powders.

UV and visible light irradiation. The MB has greater removal efficiency overall than pyrene which could be probably due to the ease of adsorption of MB on the catalyst surface compared to pyrene as evident in the Langmuir isotherms. However, the higher removal of MB and pyrene on the coated zeolite compared to the PN powders, despite the higher monolayer adsorption capacities of the PN powders, are due to the relatively greater mass of zeolite present, covering the entire surface of the petri dish used in the batch experiments.

3.3. Column test results for pyrene

Fig. 10 shows the results of the column test experiments on the photocatalytic removal of pyrene. It can be seen in Fig. 10a that during the initial stages of the column operation, the effluent pyrene concentration was minimal which could signify that pyrene was adsorbed on the column media as it passes through the height of the column. Pyrene could have been separated by means of precipitation because of its low solubility in water.

However, the precipitated pyrene rapidly saturated causing a column breakthrough which was indicated by a rise in the pyrene concentration as the volume treated increased. The column test result for low pyrene concentration is shown

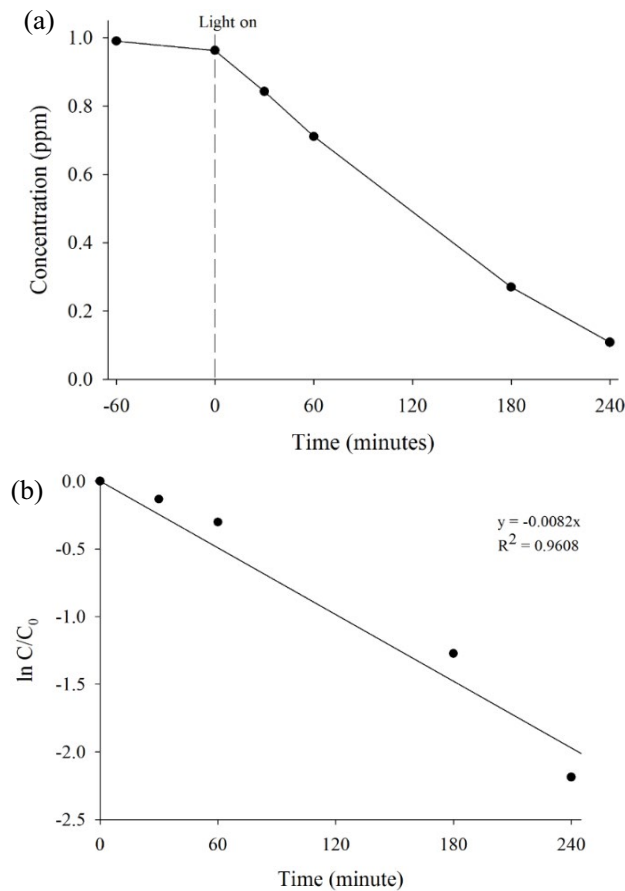


Fig. 7. (a) Concentration profile of the photocatalytic removal of pyrene using TiO_2 coated zeolite and (b) reaction kinetics of the photocatalytic removal of pyrene using TiO_2 coated zeolite.

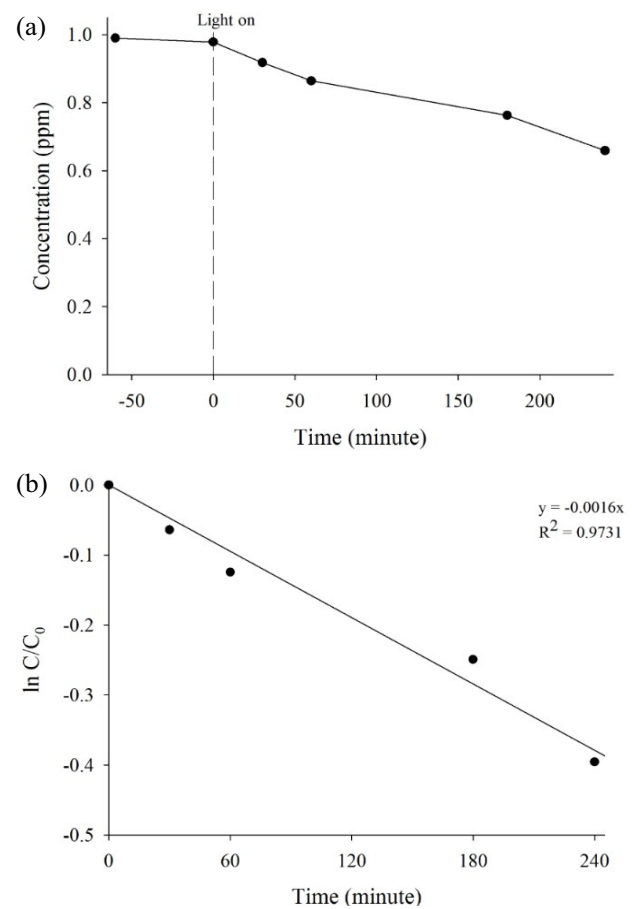


Fig. 8. (a) Concentration profile of the photocatalytic removal of pyrene using WO_3/TiO_2 powders and (b) reaction kinetics of the photocatalytic removal of pyrene using WO_3/TiO_2 powders.

Table 3

Removal efficiencies for pyrene and methylene blue using various photocatalyst types and irradiation sources

Photocatalyst	%R.E. (MB)	%R.E. (pyrene)	Light source
TiO_2 powders	86.11%	78.98%	UV-A lamps
TiO_2 coated zeolite	96.79%	88.76%	UV-A lamps
WO_3/TiO_2 powders	80.98%	32.67%	White fluorescent lamps
WO_3/TiO_2 coated zeolite	96.44%	63.28%	White fluorescent lamps

in Fig. 10b. Based on the result, ~50% of the pyrene concentration has been adsorbed on the column media regardless of the volume treated. This could be possibly due to the slow adsorption of pyrene on the surface of the coated zeolite as seen in the adsorption isotherms on the previous section. There could be also a possibility of shorter retention times of pyrene on the column resulting in the relatively lower removal efficiency of pyrene, and longer column operations would be impractical now to verify the adsorption equilibrium of pyrene on the catalyst surface, and thus these are recommended as a future study.

Lamichhane et al. [4] have reported that carbon-based adsorbents such as biochar, activated carbon, and zeolite

modified with surfactant-ion exchange capabilities can adsorb up to 98% of the PAHs such as pyrene, phenanthrene, fluorene, and fluoranthene in aqueous solutions. Therefore, PAHs have a higher affinity to organic-based adsorbents as compared to the inorganic ones such as sand and zeolite.

4. Conclusions and recommendations

The photocatalytic removal of organic compounds such as methylene blue and pyrene have been compared in this study. The photocatalytic removal of methylene blue is relatively more efficient compared to that of the photocatalytic removal of pyrene using TiO_2 and WO_3/TiO_2 powders and

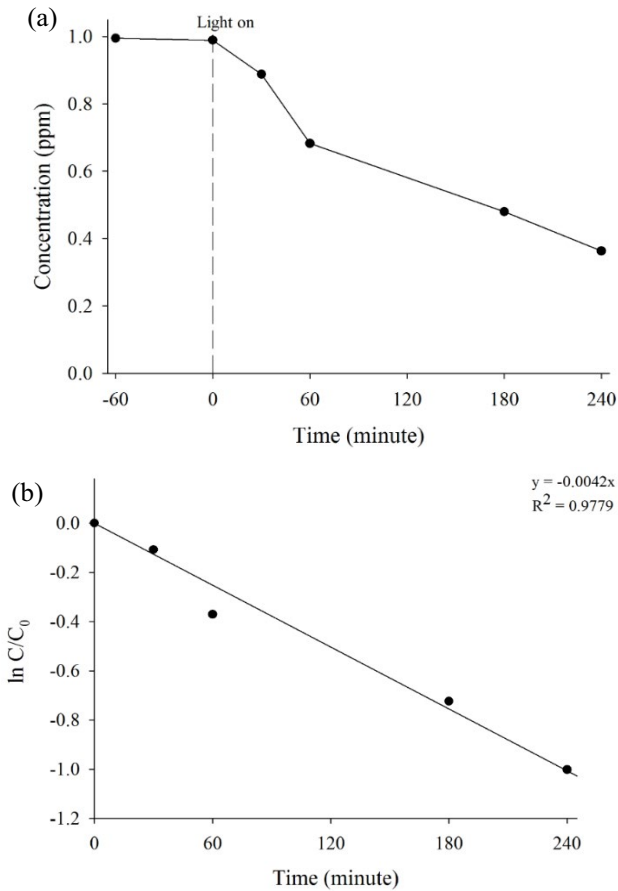


Fig. 9. (a) Concentration profile of the photocatalytic removal of pyrene using WO_3/TiO_2 coated zeolite and (b) reaction kinetics of the photocatalytic removal of pyrene using WO_3/TiO_2 coated zeolite.

TiO_2 and WO_3/TiO_2 coated zeolite. The efficient removal of MB over pyrene could be attributed to the cationic nature of MB on aqueous solutions which are readily adsorbed through electrostatic interactions on the catalyst surface due to the highly negative charge present. The ease of adsorption of MB has resulted in greater photocatalytic removal efficiency. While for the case of pyrene, it is relatively challenging for TiO_2 and WO_3/TiO_2 to adsorb pyrene on its surface due to the highly localized electrons of the aromatic part of pyrene. The generation of OH radicals from the adsorbed water could break down the stable bonds between the benzene rings of pyrene to transform it into a more positive specie which could interact with the electronegative portion of the catalyst surface. However, it would be a rate-limiting step, relative to the MB photocatalytic reaction, for the pyrene degradation process. On the other hand, the removal of pyrene under visible light irradiation proceeds at a slower rate than under UV irradiation possibly due to the higher photon energy emitted by UV than those emitted by visible light. The column test results show that pyrene at high concentrations is removed via precipitation mechanism due to the poor solubility of pyrene in water which then accumulates in the entire column resulting in faster column saturation. At lower concentrations, pyrene tends to be removed to a certain extent (~50%)

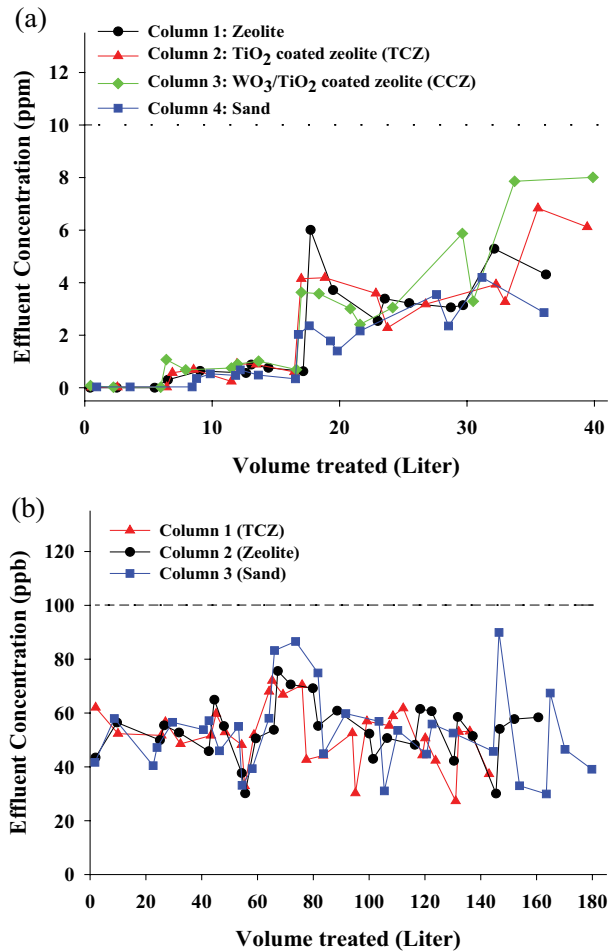


Fig. 10. (a) Column test results for an 18 d period (10 ppm pyrene concentration) and (b) column test results for a 20 d period (0.1 ppm pyrene concentration).

due to the slow adsorption of pyrene to the catalyst surface, or shorter retention times on the column. Further studies are recommended to verify the adsorption equilibrium, and effects of retention times to enhance pyrene removal on the inorganic catalysts such as zeolite, TiO_2 , and WO_3/TiO_2 . On the other hand, this study provides a significant contribution to the field of urban water quality management by presenting a cost-effective treatment for emerging pollutants such as methylene blue and pyrene.

Acknowledgment

This research was supported by the National Research Foundation (NRF-2018R1D1A1B07041093) of the Korean government.

References

[1] Z.J. Zhang, W.H. Wang, M. Shang, W.Z. Yin, Photocatalytic degradation of rhodamine B and phenol by solution combustion synthesized $BiVO_4$ photocatalyst, *Catal. Commun.*, 11 (2010) 982–986.

- [2] W. Subramonian, T.Y. Wu, Effect of enhancers and inhibitors on photocatalytic sunlight treatment of methylene blue, *Water Air Soil Pollut.*, 225 (2014) 1–15.
- [3] N. Soltani, E. Saion, W. Mahmood Mat Yunus, M. Navasery, G. Bahmanrokh, M. Erfani, M.R. Zare, E. Gharibshahi, Photocatalytic degradation of methylene blue under visible light using PVP-capped ZnS and CdS nanoparticles, *Sol. Energy*, 97 (2013) 147–154.
- [4] S. Lamichhane, K.C. Bal Krishna, R. Sarukkalige, Polycyclic aromatic hydrocarbons (PAHs) removal by sorption: a review, *Chemosphere*, 148 (2016) 336–353.
- [5] Ö. Kerkez, İ. Boz, Efficient removal of methylene blue by photocatalytic degradation with TiO₂ nanorod array thin films, *React. Kinet. Mech. Catal.*, 110 (2013) 543–557.
- [6] K. Pirkanniemi, M. Sillanpää, Heterogeneous water phase catalysis as an environmental application: a review, *Chemosphere*, 48 (2002) 1047–1060.
- [7] D. Spasiano, R. Marotta, S. Malato, P. Fernandez-Ibañez, I. Di Somma, Solar photocatalysis: materials, reactors, some commercial, and pre-industrialized applications. A comprehensive approach, *Appl. Catal., B*, 170–171 (2015) 90–123.
- [8] S.L. Bai, H.Y. Liu, J.H. Sun, Y. Tian, S. Chen, J.L. Song, R.X. Luo, D.Q. Li, A.F. Chen, C.-C. Liu, Improvement of TiO₂ photocatalytic properties under visible light by WO₃/TiO₂ and MoO₃/TiO₂ composites, *Appl. Surf. Sci.*, 338 (2015) 61–68.
- [9] J.A. Mendoza, D.H. Lee, L.-H. Kim, I.H. Kim, J.-H. Kang, Photocatalytic performance of TiO₂ and WO₃/TiO₂ nanoparticles coated on urban green infrastructure materials in removing nitrogen oxide, *Int. J. Environ. Sci. Technol.*, 15 (2018) 581–592.
- [10] A. Mills, An overview of the methylene blue ISO test for assessing the activities of photocatalytic films, *Appl. Catal., B*, 128 (2012) 144–149.
- [11] U.S. EPA, Method 3535A (SW-846): Solid-Phase Extraction (SPE), Revision 1, Washington, DC, 2007.
- [12] S. Kohtani, M. Tomohiro, K. Tokumura, R. Nakagaki, Photooxidation reactions of polycyclic aromatic hydrocarbons over pure and Ag-loaded BiVO₄ photocatalysts, *Appl. Catal., B*, 58 (2005) 265–272.